Int J Clin Exp Med 2025;18(5):112-121
www.ijcem.com /ISSN:1940-5901/IJCEM0163158

Original Article

Bioinformatic identification of Hub genes and related transcription factors in post-intracerebral hemorrhage neuroinflammation

Zhixing Hong, Junming Li, Mingrui Qiu

Department of Emergency Medicine, The First People's Hospital of Linping District, Hangzhou 311100, Zhejiang, China

Received January 7, 2025; Accepted April 6, 2025; Epub May 15, 2025; Published May 30, 2025

Abstract: Background: Neuroinflammation typically arises within 24 to 72 hours following intracerebral hemorrhage, ultimately contributing to neuronal cell apoptosis. Objective: Our objective was to integrate clinical research data and investigate new signaling pathways of ferroptosis in post-intracerebral hemorrhage neuroinflammation. Methods: We downloaded GSE125512 and identified 30 ferroptosis-related differentially expressed genes by intersecting with known ferroptosis genes. The protein-protein interaction network was performed by the STRING database and Cytoscape software to generate an interaction network among ferroptosis-related differentially expressed genes and to screen key nodes for biomarker prediction. Results: The interleukin-18 signaling pathway exhibited a statistically significant upregulation when comparing the periods of 0 to 24 hours and 72 to 96 hours post-intracerebral hemorrhage. We identified key genes associated with the interleukin-18 signaling pathway, including SQSTM1, IL-1B, and TLR4, and constructed a transcription factor-mRNA-miRNA regulatory network to pinpoint target microRNAs. Conclusion: Interleukin-18 signaling pathway activates in post-intracerebral hemorrhage neuroinflammation. Through a comprehensive bioinformatics analysis, we uncovered transcription factors and microRNA linked to interleukin-18, which offers new therapeutic targets for post-intracerebral hemorrhage neuroinflammation.

Keywords: Intracerebral hemorrhage, neuroinflammation, ferroptosis, interleukin-18

Introduction

Intracerebral hemorrhage (ICH) ranks as the second most prevalent etiology of stroke, resulting in significant morbidity and mortality [1]. According to The Global Burden of Diseases, Injuries, and Risk Factors Study, ICH constituted 27.9% of all newly identified strokes in 2019 [2]. In 2020, ICH accounted for 14.9% of stroke presentations in China [3]. Notably, fever oc curs in 30-45% of patients within the initial 72 hours following ICH onset [4]. Numerous studies indicate that neuroinflammation plays a pivotal role in the neuronal cell death associated with ICH [5, 6]. Future investigations are essential to identify key immune factors or pathways that could elucidate critical mediators of pathology in ICH.

The mechanisms of cell death in ICH encompass necroptosis, pyroptosis, ferroptosis, and autophagy [7]. Ferroptosis is characterized by the accumulation of high levels of iron ions, lipid peroxidation, and increased reactive oxygen species [8]. GPX4 is an enzyme known to inhibit ferroptosis [9]. In contrast, RSL3 antagonizes GPX4 activity, which diminishes the cellular antioxidant capacity and leads to an accumulation of reactive oxygen species, ultimately resulting in ferroptosis [10, 11]. Research has shown that the regulation of ferroptosis can be modulated by GPX4 through targeting specific immune-related proteins or genes. Notably, the knockdown of NLRP3 inflammasomes was shown to inhibit ferroptosis through this mechanism, accompanied by reduced levels of IL-18 and IL-1β [12].

Interleukin-18 (IL-18) is a pro-inflammatory cytokine that is believed to play a role in inflammation associated with various neurological diseases, including ischemic stroke, post-stroke depression, and ICH. Research has shown that knocking out IL-18 leads to a reduction in

activated microglia in ICH model mice [13]. Several studies have explored the mechanisms behind the activation of the IL-18 signaling pathway following ICH. One key aspect is pyroptosis, a form of programmed cell death that occurs after ICH, which releases IL-18 and triggers a secondary immune-inflammatory response [14]. Additionally, the NLRC4 inflammasome is involved in processing IL-18, contributing to inflammatory injury after ICH [15]. Given these findings, targeting IL-18 holds therapeutic potential for treating neuroinflammation after ICH.

The mechanisms underlying ferroptosis in neuroinflammation are currently not well understood. Given that IL-18 may play a role in post-ICH neuroinflammation, we aimed to investigate whether ferroptosis during ICH leads to the upregulation of IL-18 and to explore therapeutic strategies targeting IL-18. We began by comparing gene expression in peripheral blood samples collected from ICH patients at two different time points: 0 to 24 hours and 72 to 96 hours after the onset of symptoms. This analysis revealed 521 differentially expressed genes (DEGs). We then intersected these DEGs with a ferroptosis dataset, which led to the identification of 30 ferroptosis-related differentially expressed genes (FDEGs). Furthermore, we developed a transcription factor-mRNA-miRNA network to explore potential key biomarkers contributing to neuroinflammation following ICH. These findings provide valuable insights into the critical pathways associated with neuroinflammation after ICH and enhance our understanding of therapeutic strategies for treating this condition.

Methods

Differential expression analysis

Limma (linear models for microarray data) is a differential expression screening method based on a generalized linear model [16]. Here, we used the R software package limma (version 3.40.6) for differential analysis to obtain differential expression genes (DEGs) between different groups. First of all, the raw data GSE125512 of intracerebral hemorrhage was downloaded from Gene Expression Omnibus (GEO) [17]. Subsequently, we used the limit function to perform multiple linear regression. Further, the eBays function was used to compute moderated t-statistics, moderated F-statistics, and log-odds of differential expression by empirical Bayes moderation of the standard errors towards a common value. We considered $P < 0.05$ to be statistically significant.

The Ferroptosis Database

(http://www.zhounan.org/ferrdb/current/operations/download.html) included 534 genes also obtained to be intersected with GSE125512 to identify ferroptosis-related differentially expressed genes (FDEGs).

Functional enrichment of differentially expressed genes

To better demonstrate the biological function of DEGs, we used GO analysis in R package org.Hs.eg.db (version 3.1.0) as a background, mapped the genes to the background set, and performed enrichment analysis using clusterProfiler (version 3.14.3). The minimum number of gene sets was set to be 5 and the maximum was set to be 5000. GO terms with $P < 0.05$ and FDR < 0.05 were considered statistically significant.

To further capture the relationships between the terms, a subset of enriched terms has been selected and rendered as a network plot, where terms with a similarity > 0.3 are connected by edges. We selected the terms with the best *p*-values from each of the 20 clusters, with the constraint that there are no more than 15 terms per cluster and no more than 250 terms in total. The network is visualized using Cytoscape5, where each node represents an enriched term and is colored first by its cluster-ID and then by its *p*-value.

Protein-protein interaction network analysis

STRING (https://string-db.org/) is an online database to study protein-protein interaction information [18]. In the paper, we set the default cutoff (interaction score > 0.4) in the STRING online database. Genes were represented by nodes, and the interactions between the genes were indicated by edges. Furthermore, the functional analysis for genes using Metascape.

Gene-miRNA interaction networks

We used TRRUST version 2 (https://www.grnpedia.org/trrust/) to obtain the T-mRNA relationship pair data [19] and used miRWalk (http://mirwalk.umm.uni-heidelberg.de/) to ex-

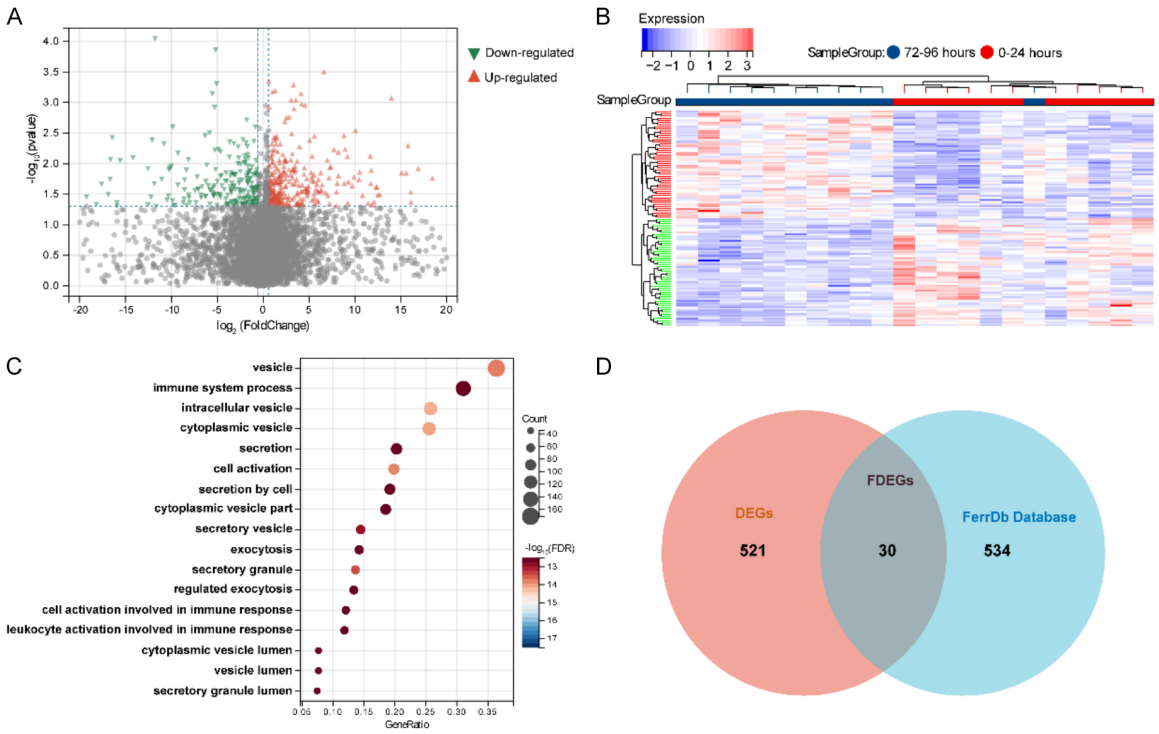

Figure 1. Identification and classification of differentially expressed genes in IHC samples. A: Volcano plot showing differentially expressed genes (DGEs) in the dataset GSE125512. Red dots represent up-regulated genes and green dots represent down-regulated genes. B: An expression heat map of the DEGs in the GSE125512 dataset. Red color represented up-regulated genes and blue color represented down-regulated genes. C: GO enrichment analysis of DEGs with bar-plot. The dot size reflects the number of genes enriched under the given ontology term, and the color indicates the significance of enrichment. D: Venn diagram of ferroptosis-related differentially expressed genes (FDEGs). The Ferroptosis dataset is intersected with GSE125512 to identify FDEGs.

plore the gene-miRNA interaction networks [20]. In addition, we screened key transcription factors that overlapped more than 2 genes and miRNAs that target more than two genes.

Results

Ferroptosis-related genes are upregulated in the periods of 72 to 96 hours post-intracerebral hemorrhage

We downloaded GSE125512 from the GEO database and identified a total of 551 differentially expressed genes (DEGs) in the peripheral blood gene expression induced by intracerebral hemorrhage (ICH) at 72 to 96 hours compared to 0 to 24 hours. This included 311 upregulated genes and 240 downregulated genes. The heat map and volcano plot of the DEGs are shown in **Figure 1A** and **1B**. Furthermore, we conducted a Gene Ontology (GO) enrichment analysis to reveal the potential biological significance of these DEGs. The upregulated DEGs were primarily involved in immune system processes, intracellular vesicles, cytoplasmic vesicles, secretion, and cell activation (**Figure 1C**). Next, we intersected these DEGs with 564 ferroptosis-related genes obtained from the FerrDb database. The Venn diagram illustrates 30 ferroptosis-related differentially expressed genes (FDEGs) that are common between the two datasets (**Figure 1D**), comprising 16 upregulated and 14 downregulated genes (**Table 1**). These FDEGs were further classified as ferroptosis drivers, ferroptosis suppressors, and ferroptosis markers (**Table 2**). Among the findings, two suppressors - TMSB4X and FTL-exhibited significant upregulation, while TLR2 and MAPK were significantly downregulated, indicating the activation of inhibitory pathways during the 72 to 96 hours post-ICH period. However, the ferroptosis marker NFE2L2 remained upregulated, alongside the sustained release of the cytokine IL-1β, suggesting ongoing neuroinflammation and ferroptosis. The results showed that an anti-inflammatory process occurs in parallel with neuroinflammation in post-ICH neuroinflammation.

Table 1. Ferroptosis-related differentially expressed genes of intracerebral hemorrhage

Gene symbol	*P*-value	logFC	Gene name	Gene ID
TMSB4X	0.0161105	832.315909	thymosin beta 4, X-linked	7114
FTL	0.02654884	491.93873	ferritin light chain	2512
CYBB	0.0084075	86.6314706	cytochrome b-245 beta chain	1536
CTSB	0.03142506	23.8354833	cathepsin B	1508
CFL1	0.0141053	15.0749937	cofilin 1	1072
IL1B	0.01825334	10.4426286	interleukin 1 beta	3553
SQSTM1	0.04401366	9.21699755	sequestosome 1	8878
BID	0.0058005	8.92396907	BH3 interacting domain death agonist	637
TRIM21	0.00646655	8.18493467	tripartite motif containing 21	6737
TIMP1	0.03703792	5.55847592	TIMP metallopeptidase inhibitor 1	7076
NFE2L2	0.00071917	4.13110903	nuclear factor, erythroid 2 like 2	4780
CHP1	0.04611212	3.59918755	calcineurin like EF-hand protein 1	11261
CS	0.03858287	1.94544291	citrate synthase	1431
FADS1	0.0469293	1.08097498	fatty acid desaturase 1	3992
SREBF2	0.04617337	0.69159975	sterol regulatory element binding transcription factor 2	6721
MYB	0.02267785	0.62078398	MYB proto-oncogene, transcription factor	4602
TLR4	0.02651365	-104.38385	toll like receptor 4	7099
PARP8	0.01807284	-16.656838	poly (ADP-ribose) polymerase family member 8	79668
MIR15A	0.00378213	-16.450918	microRNA 15a	406948
ZFAS1	0.03554356	-12.228215	ZNFX1 antisense RNA 1	441951
RICTOR	0.03381748	-10.32279	RPTOR independent companion of MTOR complex 2	253260
GABARAPL1	0.01260636	-10.277444	GABA type A receptor associated protein like 1	23710
OSBPL9	0.00351135	-6.3200169	oxysterol binding protein like 9	114883
CIRBP	0.02719321	-5.7287768	cold inducible RNA binding protein	1153
MIR302A	0.01539279	-3.0732534	microRNA 302a	407028
ACSL3	0.04586207	-2.2655125	acyl-CoA synthetase long-chain family member 3	2181
DDIT3	0.01413426	-1.6724347	DNA damage inducible transcript 3	1649
EMC2	0.01304393	-1.4298627	ER membrane protein complex subunit 2	9694
FANCD2	0.03830996	-1.0412744	Fanconi anemia complementation group D2	2177
MAPK8	0.01564312	-0.5887148	mitogen-activated protein kinase 8	5599

Table 2. The ferroptosis-related differentially expressed genes were classified into ferroptosis driver, suppressor, and marker

Suppressor	Driver	Marker
NFE2L2, TMSB4X, PARP8, FTL, RICTOR, FANCD2, SQSTM1, ACSL3, SREBF2	OSBPL9, MIR15A, BID, TRIM21, CYBB, GABARAPL1, EMC2, CFL1, MIR302A, MAPK8, IL1B, MYB, TLR4, CIRBP, CTSB, ZFAS1, TIMP1, CS, CHP1, FADS1	NFE2L2

IL-18 signal pathway activates in post-intracerebral hemorrhage neuroinflammation

We utilized 30 FDEGs to perform Gene Ontology (GO) analysis using the Metascape online platform. The findings indicated that these genes were mainly enriched in processes related to necroptosis, cellular response to external stimulus, and cellular response to chemical stress (**Figure 2**), which revealed that cellular signal pathways were induced by biological stimulus. Therefore, ER-nucleus signal pathway, ferroptosis, IL-18 signal pathway and HIF-1 signal pathway exhibited significant activation (**Figure 2**).

Protein-protein interaction network analysis of ferroptosis-related differentially expressed genes

In order to investigate the mechanistic signaling program that underly pro-inflammatory activation, we established a protein-protein inter-

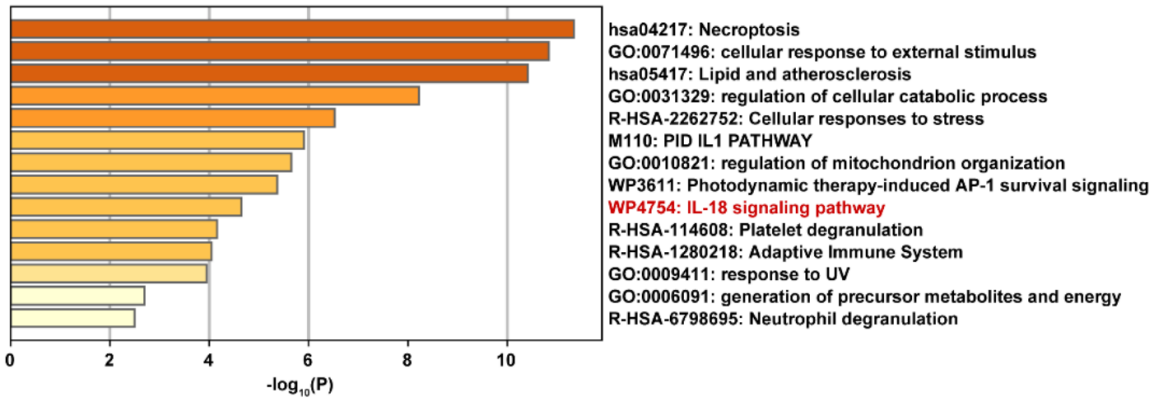

Figure 2. Enrichment pathway of ferroptosis-related differentially expressed genes. Metascape chart of top 20 biological pathways. Each band represents the enriched term or pathway colored by *p*-value.

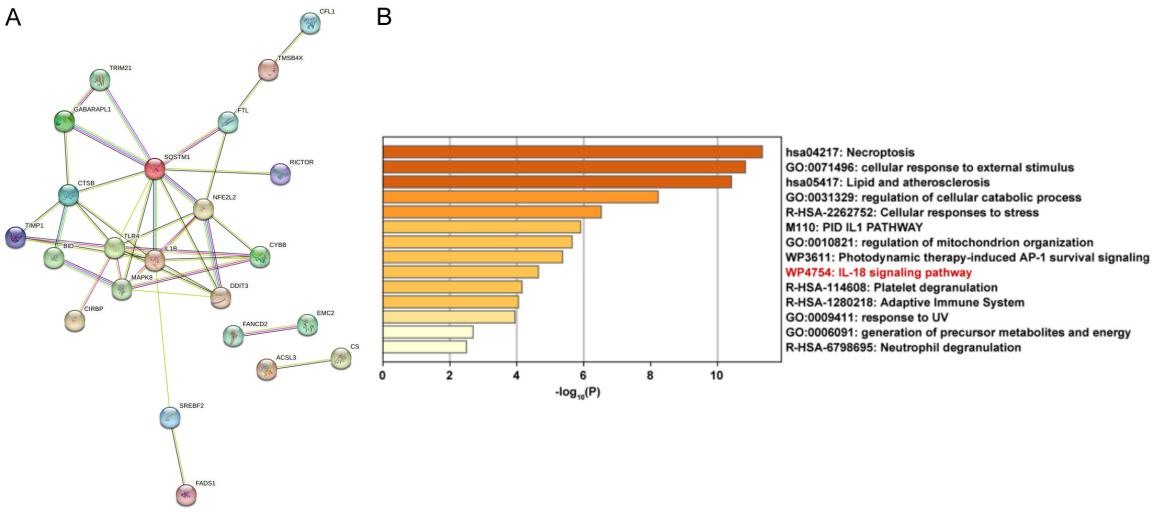

Figure 3. Protein-Protein Interaction Network Analysis of ferroptosis-related differentially expressed genes. A: The protein-protein interaction network constructed among FDEGs. Genes were represented by nodes, and the interactions between the genes were indicated by edges. B: Functional enrichment analysis.

action network to identify potential interacting proteins associated with the IL-18 signaling pathway. Notably, SQSTM1, IL-1B, and TLR4 may significant impact this pathway (**Figure 3A**). Furthermore, GO analysis demonstrated that these genes are enriched in the PID IL1 pathway, the IL-18 signaling pathway, and the adaptive immune system (**Figure 3B**).

MiRNA interaction of ferroptosis-related differentially expressed genes

TRRUST database was used to contrasted transcription factor (TF)-mRNA-miRNA intersection network, which was helpful to find key transcription factors and targeted miRNA. Through the use of the TRRUST database, a total of 12 significant TFs and 94 miRNAs were identified (**Figure 4A**). Among 12 key TFs, 8 were found to target IL1B (**Table 3**). Additionally, there were 7 miRNAs that received a score of ≥2 (**Table 4**). These miRNAs were primarily enriched in transcription factor activity, kinase activity, and receptor binding. The principal biological pathways implicated in this analysis included the glypican pathway, the ErbB receptor signaling network, and plasma membrane estrogen receptor signaling (**Figure 4B**).

Discussion

This study utilized bioinformatics methods to identify crucial genes involved in ferroptosis related to neuroinflammation following intracere-

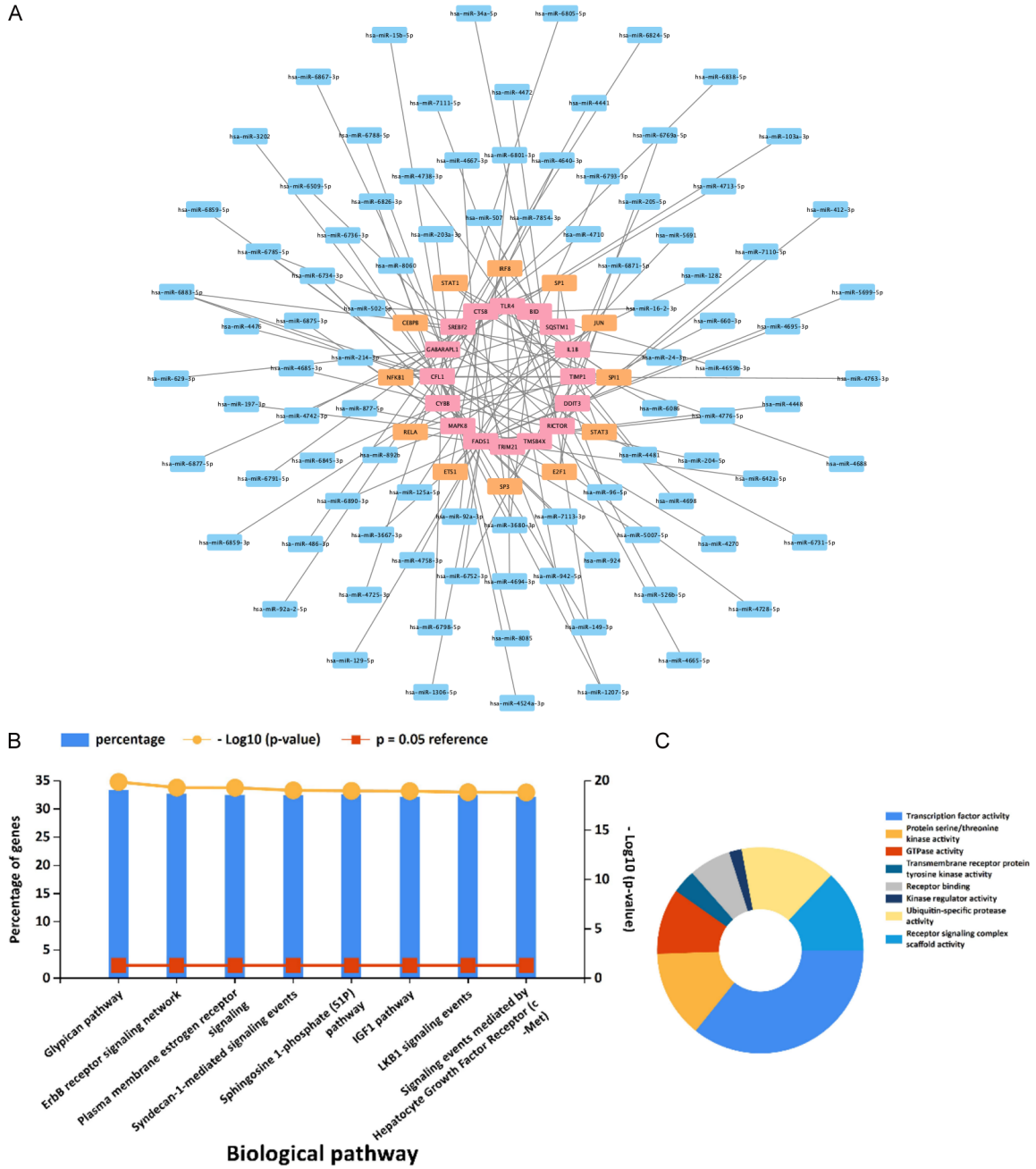

Figure 4. MiRNA Interaction of ferroptosis-related differentially expressed genes. (A) The transcription factor-mRNA-miRNA network among FDEGs. Pink: FDEGs. Yellow: TFs. Blue: miRNAs. The edge represents different relationships. (B) The biological pathways and (C) molecular function of miRNAs.

bral hemorrhage (ICH) and explored the underlying mechanisms. We successfully identified 30 ferroptosis-related differentially expressed genes (FDEGs) by intersecting the differentially expressed genes (DEGs) from datasets GSE-125512 with those from the Ferroptosis Database. The results of pathway enrichment analysis of FDEGs and protein-protein interaction (PPI) networks suggested that the IL-18 signaling pathway plays a significant role in post-ICH neuroinflammation. Furthermore, we identified several genes associated with the IL-18 signaling pathway, including IL-1β and TLR4. We also recognized key transcription factors and targeted microRNAs using the TRRUST database. This study provides valuable insights into the

Table 3. Key transcription factors and their target genes

Key TF	Count	*P* value	List of overlapped genes
IRF8	3	1.42E-07	CYBB, IL1B, TLR4
NFKB1	5	9.97E-06	TRIM21, IL1B, CTSB, TIMP1, SQSTM1
SPI1	3	3.15E-05	IL1B, CYBB, TLR4
STAT1	3	7.83E-05	CTSB, TIMP1, IL1B
RELA	4	0.000203	IL1B, CTSB, TIMP1, TRIM21
E2F1	3	0.000312	IL1B, MAPK8, DDIT3
JUN	3	0.000426	MAPK8, IL1B, DDIT3
CEBPB	2	0.00164	IL1B, DDIT3
ETS1	2	0.00283	CTSB, SQSTM1
SP3	2	0.00569	TIMP1, CTSB
STAT3	2	0.00884	TIMP1, DDIT3
SP1	3	0.0112	CTSB, SQSTM1, TIMP1

Table 4. miRNAs and its target genes

miRNA ID	Gene targeted by miRNA	Count
hsa-miR-1207-5p	SREBF2, CFL1	2
hsa-miR-149-3p	RICTOR, CFL1	2
hsa-miR-3680-3p	BID, MAPK8	2
hsa-miR-6734-3p	CYBB, FADS1	2
hsa-miR-6752-3p	FADS1, TMSB4X	2
hsa-miR-6785-5p	SREBF2, CFL1	2
hsa-miR-6883-5p	RICTOR, SREBF2, CFL1	3

mechanisms through which IL-18 influences ICH from a bioinformatics perspective.

IL-18 is a pro-inflammatory cytokine located on chromosome 11 in humans, consisting of 7 exons [21]. The transcription of the IL-18 precursor is activated under certain conditions, such as when pathogen-associated molecular patterns (PAMPs) bind to Toll-like receptors (TLRs) or through the activation of the NF-κB signaling pathway [22]. The IL-18 precursor is cleaved by caspase 1 and released as mature IL-18 [23]. Once released, IL-18 binds to IL-18Rα, forming a signaling complex that recruits IL-18Rβ [24]. The formation of this heterodimer allows MyD88 to bind to the TIR domain of IL-18Rα and IL-18Rβ, initiating the IL-18 signaling cascade. This cascade ultimately leads to the translocation of NF-κB into the nucleus [25]. IL-18 activates microglia to modulate the inflammatory response after ICH [13]. Previous investigations have predominantly concentrated on the involvement of IL-18 in ICH through the inflammasome [15, 26].

Ferroptosis is known to be associated with the release of pro-inflammatory molecules, such as IL-18. However, current research has not definitively established a direct causal relationship between ferroptosis and IL-18. Many studies suggest a potential connection between the two. Notably, ferroptosis is linked to the activation of the NLRP3 inflammasome, which indirectly leads to the release of IL-18 [27]. Additionally, high iron stress during ferroptosis has been shown to upregulate the expression of IL-18 [28]. In this context, we aim to explore the relationship between IL-18 and ferroptosis, proposing that the IL-18 signaling pathway may regulate ferroptosis in post-ICH neuroinflammation.

The genes from 30 FDEGs identified to be involved in the IL-18 pathway included BID, IL1B, and TIMP1. BID, a pro-apoptotic *Bcl-2* family member [29], is activated through cleaving by caspase 8, which subsequently promotes the release of cytochrome C from the mitochondria [30, 31]. IL-18 triggers cell death through the action of BID and the subsequent release of cytochrome C in endothelial cells [32]. Both IL-1β and IL-18 generally induced pyroptosis via inflammasomes [33]. TIMP1 is a member of the family of tissue inhibitors of metalloproteinases. A study has shown that loss of TIMP1 reduced the expression of GPX4, which increased the level of ferroptosis [34]. These findings suggest that these genes are all implicated in the regulation of cell death. While our investigation did not delve deeper into the mechanisms by which these genes influence ferroptosis, we have established their direct link to this form of cell death.

Transcription factors modulate gene expression and play an essential role in nearly all physiological processes. We constructed the TF-mRNA-miRNA network to pinpoint the critical TFs. Among the twelve key TFs identified, eight were found to target IL1B, which include IRF8, NFKB1, SPI1, STAT1, RELA, E2F1, JUN, and CEBPB. The melanocortin-1 receptor was observed to mitigate neuroinflammation via the

CREB/Nr4a1/NF-κB signaling pathway following ICH in mice [35]. Spi1, which encodes the PU.1 protein, regulates the microglial inflammatory response after intracerebral hemorrhage via PI3K/AKT/mTOR [36]. Additionally, STAT1 elevates the transcription of Trpm7 via H3K27ac, resulting in calcium overload post-ICH [37]. Moreover, curcumin has been shown to reduce neuroinflammation after IHC by inhibiting the JAK1/STAT1 pathway [38]. Therefore, alongside the induction of ferroptosis, these TFs exacerbate IHC through various other pathways.

In this research, we identified several genes and transcription factors associated with ferroptosis during neuroinflammation following ICH. Many of these genes and transcription factors have not been explored in previous studies. Our analysis focused specifically on the IL-18 signaling pathway. We screened for genes related to IL-18 and identified key target transcription factors. Additionally, we identified seven targeted microRNAs that may serve as promising novel biomarkers.

One limitation of this study is the relatively small sample size, which may restrict the generalizability of the results. Additionally, our findings focus solely on the relationship between ferroptosis and IL-18. It is important to note that ferroptosis in the context of post-ICH does not directly contribute to the upregulation of IL-18. Further research is needed in this area. For instance, inflammasome activation plays a role in the processing of IL-18, which can worsen brain injury during post-ICH neuroinflammation. Therefore, future studies should explore various upstream signaling pathways that are involved in the upregulation of IL-18.

Disclosure of conflict of interest

None.

Address correspondence to: Zhixing Hong, Department of Emergency Medicine, The First People's Hospital of Linping District, Hangzhou 311100, Zhejiang, China. E-mail: tutu05052024@163.com

References

[1] Magid-Bernstein J, Girard R, Polster S, Srinath A, Romanos S, Awad IA and Sansing LH. Cerebral hemorrhage: pathophysiology, treatment, and future directions. Circ Res 2022; 130: 1204-1229.

[2] GBD 2019 Stroke Collaborators. Global, regional, and national burden of stroke and its risk factors, 1990-2019: a systematic analysis for the Global Burden of Disease Study 2019. Lancet Neurol 2021; 20: 795-820.

[3] Tu WJ and Wang LD; Special Writing Group of China Stroke Surveillance Report. China stroke surveillance report 2021. Mil Med Res 2023; 10: 33.

[4] Schwarz S, Hafner K, Aschoff A and Schwab S. Incidence and prognostic significance of fever following intracerebral hemorrhage. Neurology 2000; 54: 354-61.

[5] Lan X, Han X, Liu X and Wang J. Inflammatory responses after intracerebral hemorrhage: from cellular function to therapeutic targets. J Cereb Blood Flow Metab 2019; 39: 184-186.

[6] Mracsko E and Veltkamp R. Neuroinflammation after intracerebral hemorrhage. Front Cell Neurosci 2014; 8: 388.

[7] Zhang Y, Khan S, Liu Y, Zhang R, Li H, Wu G, Tang Z, Xue M and Yong VW. Modes of brain cell death following intracerebral hemorrhage. Front Cell Neurosci 2022; 16: 799753.

[8] Dixon SJ, Lemberg KM, Lamprecht MR, Skouta R, Zaitsev EM, Gleason CE, Patel DN, Bauer AJ, Cantley AM, Yang WS, Morrison B 3rd and Stockwell BR. Ferroptosis: an iron-dependent form of nonapoptotic cell death. Cell 2012; 149: 1060-72.

[9] Stockwell BR, Friedmann Angeli JP, Bayir H, Bush AI, Conrad M, Dixon SJ, Fulda S, Gascon S, Hatzios SK, Kagan VE, Noel K, Jiang X, Linkermann A, Murphy ME, Overholtzer M, Oyagi A, Pagnussat GC, Park J, Ran Q, Rosenfeld CS, Salnikow K, Tang D, Torti FM, Torti SV, Toyokuni S, Woerpel KA and Zhang DD. Ferroptosis: a regulated cell death nexus linking metabolism, redox biology, and disease. Cell 2017; 171: 273-285.

[10] Li S, He Y, Chen K, Sun J, Zhang L, He Y, Yu H and Li Q. RSL3 drives ferroptosis through NF-kappaB pathway activation and GPX4 depletion in Glioblastoma. Oxid Med Cell Longev 2021; 2021: 2915019.

[11] Sui X, Zhang R, Liu S, Duan T, Zhai L, Zhang M, Han X, Xiang Y, Huang X, Lin H and Xie T. RSL3 drives ferroptosis through GPX4 inactivation and ROS production in colorectal cancer. Front Pharmacol 2018; 9: 1371.

[12] Wang Z, Li Y, Ye Y, Zhu H, Zhang J, Wang H, Lei J, Gu L and Zhan L. NLRP3 inflammasome deficiency attenuates cerebral ischemia-reperfusion injury by inhibiting ferroptosis. Brain Res Bull 2023; 193: 37-46.

[13] Li H, Tian J, Yin Y, Diao S, Zhang X, Zuo T, Miao Z and Yang Y. Interleukin-18 mediated inflammatory brain injury after intracerebral hemorrhage in male mice. J Neurosci Res 2022; 100: 1359-1369.

[14] Song D, Yeh CT, Wang J and Guo F. Perspectives on the mechanism of pyroptosis after intracerebral hemorrhage. Front Immunol 2022; 13: 989503.
[15] Gan H, Zhang L, Chen H, Xiao H, Wang L, Zhai X, Jiang N, Liang P, Zheng S and Zhao J. The pivotal role of the NLRC4 inflammasome in neuroinflammation after intracerebral hemorrhage in rats. Exp Mol Med 2021; 53: 1807-1818.
[16] Ritchie ME, Phipson B, Wu D, Hu Y, Law CW, Shi W and Smyth GK. limma powers differential expression analyses for RNA-sequencing and microarray studies. Nucleic Acids Res 2015; 43: e47.
[17] Walsh KB, Zhang X, Zhu X, Wohleb E, Woo D, Lu L and Adeoye O. Intracerebral hemorrhage induces inflammatory gene expression in peripheral blood: global transcriptional profiling in intracerebral hemorrhage patients. DNA Cell Biol 2019; 38: 660-669.
[18] Szklarczyk D, Morris JH, Cook H, Kuhn M, Wyder S, Simonovic M, Santos A, Doncheva NT, Roth A, Bork P, Jensen LJ and von Mering C. The STRING database in 2017: quality-controlled protein-protein association networks, made broadly accessible. Nucleic Acids Res 2017; 45: D362-D368.
[19] Han H, Cho JW, Lee S, Yun A, Kim H, Bae D, Yang S, Kim CY, Lee M, Kim E, Lee S, Kang B, Jeong D, Kim Y, Jeon HN, Jung H, Nam S, Chung M, Kim JH and Lee I. TRRUST v2: an expanded reference database of human and mouse transcriptional regulatory interactions. Nucleic Acids Res 2018; 46: D380-D386.
[20] Sticht C, De La Torre C, Parveen A and Gretz N. miRWalk: an online resource for prediction of microRNA binding sites. PLoS One 2018; 13: e0206239.
[21] Nakanishi K, Yoshimoto T, Tsutsui H and Okamura H. Interleukin-18 regulates both Th1 and Th2 responses. Annu Rev Immunol 2001; 19: 423-74.
[22] Kaplanski G. Interleukin-18: biological properties and role in disease pathogenesis. Immunol Rev 2018; 281: 138-153.
[23] Gu Y, Kuida K, Tsutsui H, Ku G, Hsiao K, Fleming MA, Hayashi N, Higashino K, Okamura H, Nakanishi K, Kurimoto M, Tanimoto T, Flavell RA, Sato V, Harding MW, Livingston DJ and Su MS. Activation of interferon-gamma inducing factor mediated by interleukin-1beta converting enzyme. Science 1997; 275: 206-9.
[24] Torigoe K, Ushio S, Okura T, Kobayashi S, Taniai M, Kunikata T, Murakami T, Sanou O, Kojima H, Fujii M, Ohta T, Ikeda M, Ikegami H and Kurimoto M. Purification and characterization of the human interleukin-18 receptor. J Biol Chem 1997; 272: 25737-42.
[25] Yasuda K, Nakanishi K and Tsutsui H. Interleukin-18 in health and disease. Int J Mol Sci 2019; 20: 649.
[26] Yao ST, Cao F, Chen JL, Chen W, Fan RM, Li G, Zeng YC, Jiao S, Xia XP, Han C and Ran QS. NLRP3 is required for complement-mediated caspase-1 and IL-1beta activation in ICH. J Mol Neurosci 2017; 61: 385-395.
[27] He Y, Wang J, Ying C, Xu KL, Luo J, Wang B, Gao J, Yin Z and Zhang Y. The interplay between ferroptosis and inflammation: therapeutic implications for cerebral ischemia-reperfusion. Front Immunol 2024; 15: 1482386.
[28] Su G, Yang W, Wang S, Geng C and Guan X. SIRT1-autophagy axis inhibits excess iron-induced ferroptosis of foam cells and subsequently increases IL-1Beta and IL-18. Biochem Biophys Res Commun 2021; 561: 33-39.
[29] Yin XM. Signal transduction mediated by Bid, a pro-death Bcl-2 family proteins, connects the death receptor and mitochondria apoptosis pathways. Cell Res 2000; 10: 161-7.
[30] Zong WX, Lindsten T, Ross AJ, MacGregor GR and Thompson CB. BH3-only proteins that bind pro-survival Bcl-2 family members fail to induce apoptosis in the absence of Bax and Bak. Genes Dev 2001; 15: 1481-6.
[31] Wei MC, Zong WX, Cheng EH, Lindsten T, Panoutsakopoulou V, Ross AJ, Roth KA, MacGregor GR, Thompson CB and Korsmeyer SJ. Proapoptotic BAX and BAK: a requisite gateway to mitochondrial dysfunction and death. Science 2001; 292: 727-30.
[32] Chandrasekar B, Vemula K, Surabhi RM, Li-Weber M, Owen-Schaub LB, Jensen LE and Mummidi S. Activation of intrinsic and extrinsic proapoptotic signaling pathways in interleukin-18-mediated human cardiac endothelial cell death. J Biol Chem 2004; 279: 20221-33.
[33] He Y, Hara H and Nunez G. Mechanism and regulation of NLRP3 inflammasome activation. Trends Biochem Sci 2016; 41: 1012-1021.
[34] Wang L, Wang J and Chen L. TIMP1 represses sorafenib-triggered ferroptosis in colorectal cancer cells by activating the PI3K/Akt signaling pathway. Immunopharmacol Immunotoxicol 2023; 45: 419-425.
[35] Wu X, Fu S, Liu Y, Luo H, Li F, Wang Y, Gao M, Cheng Y and Xie Z. NDP-MSH binding melanocortin-1 receptor ameliorates neuroinflammation and BBB disruption through CREB/Nr4a1/NF-kappaB pathway after intracerebral hemorrhage in mice. J Neuroinflammation 2019; 16: 192.
[36] Zhang G, Lu J, Zheng J, Mei S, Li H, Zhang X, Ping A, Gao S, Fang Y and Yu J. Spi1 regulates the microglial/macrophage inflammatory response via the PI3K/AKT/mTOR signaling

pathway after intracerebral hemorrhage. Neural Regen Res 2024; 19: 161-170.

[37] Li J, Ren H, Wang Y, Hoang DM, Li Y and Yao X. Mechanism of Stat1 in the neuronal Ca(2+) overload after intracerebral hemorrhage via the H3K27ac/Trpm7 axis. J Neurophysiol 2022; 128: 253-262.

[38] Wang F, Xia JJ, Shen LJ, Jiang TT, Li WL, You DL, Chang Q, Hu SY, Wang L and Wu X. Curcumin attenuates intracerebral hemorrhage-induced neuronal apoptosis and neuroinflammation by suppressing JAK1/STAT1 pathway. Biochem Cell Biol 2022; 100: 236-245.